
Eigenwavelets of the Wave Equation

Gerald Kaiser

Signals & Waves, Austin, TX www.wavelets.com kaiser@wavelets.com

Summary. We study a class of localized solutions of the wave equation, called eigenwavelets, obtained by extending its fundamental solutions to complex spacetime in the sense of hyperfunctions. The imaginary spacetime variables, which form a timelike vector, act as scale parameters generalizing the scale variable of wavelets in one dimension. They determine the shape of the wavelets in spacetime, making them pulsed beams that can be focused as tightly as desired around a single ray by letting y approach the light cone. Furthermore, the absence of any sidelobes makes them especially attractive for communications, remote sensing and other applications using acoustic waves. (A similar set of 'electromagnetic eigenwavelets' exists for Maxwell's equations.) I review the basic ideas in Minkowski space $\mathbb{R}^{3;1}$, then compute sources whose realization should make it possible to radiate and absorb such wavelets. This motivates an extension of Huygens' principle allowing equivalent sources to be represented on shells instead of surfaces surrounding a bounded source.

1 Extension of wave functions to complex spacetime

The ideas to be presented here affirm that complex analysis resonates deeply in "real" physical and geometric settings, and so they are close in spirit to the work of Carlos Berenstein (see [BG 91, BG 95, B 98] for example), to whom this volume is dedicated.

Acoustic and electromagnetic wavelets were first constructed in [K 94]. It was shown that solutions of homogeneous (i.e., sourceless) scalar and vector wave equations in Minkowski space $\mathbb{R}^{3;1}$ extend naturally to complex spacetime, and the wavelets were defined as the Riesz duals of evaluation maps acting on spaces of such holomorphic solutions. The sourceless wavelets then split naturally into retarded and advanced parts emitted and absorbed, respectively, by sources located on branch cuts needed to make these parts single-valued. Later work [K 3, K 4] was aimed at the construction of realizable source distributions which, when synthesized, would act as antennas radiating and receiving the wavelets. Two difficulties with this approach have been (a)

that the computed sources are quite singular, consisting of multiple surface layers that may be difficult to realize in practice, and (b) in the electromagnetic case the sources appeared to require a nonvanishing magnetic charge distribution, which cannot be realized as no magnetic monopoles have been observed in Nature. In this paper we resolve the first difficulty by replacing the spheroidal surface supporting the sources in [K 3, K 4] by a spheroidal shell. It is shown in [K 4a] that the second difficulty can be overcome using Hertz potentials, which give a charge-current distribution due solely to bound electric charges confined to the shell.

Although our constructions generalize to other dimensions, we shall concentrate here on the physical case of the Minkowski space $R^{3;1}$. Let

$$x = (r;t); y = (a;b) \in R^{3;1} \tag{1}$$

be real spacetime vectors and define the complex causal tube

$$T = \{x - iy \in C^4 : y \text{ is timelike, i.e., } |b| > |a|\} \tag{2}$$

It was shown in [K 94, K 3] that solutions of the homogeneous wave equation

$$\square f_0(x) = 0 \tag{3}$$

extend naturally to analytic functions $f_0(x - iy)$ in T in the sense that

$$\lim_{y \rightarrow 0^+} f_0(x - iy) = f_0(x) \tag{4}$$

where $y \rightarrow 0^+$ means that y approaches the origin within the future cone, i.e., with $b > |a|$. This kind of extension to complex domains is familiar in hyperfunction theory; see [K 88, K S99] for example. We now show that even when the wave function has a source, i.e.,

$$\square f(x) = g(x); \tag{5}$$

it extends analytically to T outside a spacetime region determined by the source. It will suffice to do this for the retarded propagator

$$G(x) = \frac{\delta(t - r)}{r}; \tag{6}$$

which is the unique causal fundamental solution:

$$\square G(x) = \delta(x); G(r;t) = 0 \text{ for } t < 0; \tag{7}$$

If the source g is supported in a compact spacetime region W , the unique causal solution of (5) is given by

$$f(x) = \int_W dx^0 G(x - x^0)g(x^0); \tag{8}$$

Assume for the moment that $G(x)$ has been extended to $G(x - iy)$. Then we define the source of G as the distribution $\tilde{\delta}$ in real spacetime given by

$$\Delta_x \tilde{\delta}(x - iy) = \Delta_x G(x - iy); \tag{9}$$

where Δ_x means that the wave operator acts only on x , in a distributional sense, so that the imaginary spacetime vector y is regarded as an auxiliary parameter. The extended solution is now defined as

$$f(x - iy) = \int_W dx^0 G(x - x^0 - iy)g(x^0) \tag{10}$$

and it satisfies the wave equation

$$\Delta_x f(x - iy) = \Delta_x g(x - iy)$$

with the extended source

$$g(x - iy) = \int_W dx^0 \tilde{\delta}(x - x^0 - iy)g(x^0); \tag{11}$$

Formally, the extended delta function $\tilde{\delta}(x - iy)$ is a 'point source' at the imaginary spacetime point iy as seen by a real observer at x . Actually, it will be seen to be a distribution in x with compact spatial (but not temporal) support localized around the spatial origin ($r = 0$) and depending on the choice of a branch cut needed to make G single-valued. This branch cut is precisely the region where G fails to be analytic, and the integral (10) determines a region W containing W where f fails to be analytic.

A general solution $f_1(x)$ of (5) is obtained by adding a sourceless wave $f_0(x)$ to (8). Since f_0 is analytic in T , f_1 is analytic in T outside of W . It therefore suffices to concentrate on the propagators as claimed. In the rest of the paper we construct extended propagators, study their properties, and compute their sources.

2 Extended propagators

In accordance with (1), we use the following notation for complex space and time variables:

$$\begin{aligned} \mathfrak{r} &= r - ia \in \mathbb{C}^3; & \mathfrak{t} &= t - ib \in \mathbb{C} \\ \mathfrak{x} &= x - iy = (\mathfrak{r}, \mathfrak{t}) \in \mathbb{T}, & \langle \mathfrak{j} | &> \langle \mathfrak{j} | \end{aligned}$$

As above, we interpret ia formally as an imaginary spatial source point, so that \mathfrak{r} is the vector from the imaginary source point ia to a real observer at r . To extend the propagator (6), begin by replacing the one-dimensional delta function with the Cauchy kernel,

$$\zeta(t) \sim \tilde{\zeta}(t) = \frac{1}{2 - it}; \quad \tau = t - ib; \tag{12}$$

which indeed satisfies a condition of type 4):

$$\lim_{b \rightarrow 0} \int_{-\infty}^{\infty} \tilde{\zeta}(t - ib) \tilde{\zeta}^*(t + ib) dt = \int_{-\infty}^{\infty} \zeta(t) dt \tag{13}$$

To complete the extension of $G(r; t)$, we must also extend the Euclidean distance $r(r) = |\mathbf{r}|$. Define the complex distance from the source to the observer as

$$\mathfrak{r}(\mathfrak{r}) = \frac{p}{r} - \frac{iq}{r^2 - a^2 - 2ir} a; \quad \text{where } r = |\mathbf{r}|, a = |\mathbf{a}| \tag{14}$$

$\mathfrak{r}(\mathfrak{r})$ is an analytic continuation to \mathbb{C}^3 of $r(r)$. Being a complex square root, it has branch points wherever $\mathfrak{r} - \mathfrak{r} = 0$. For fixed $a \neq 0$, these form a circle of radius a in the plane orthogonal to \mathbf{a} ,¹

$$C = \{ \mathfrak{r} \in \mathbb{R}^3 : \mathfrak{r} - \mathfrak{r} = 0, |\mathfrak{r} - \mathbf{a}| = a \} \tag{15}$$

To be consistent with the notation $\mathfrak{r} = p + iq$, we write

$$\mathfrak{r} = p + iq \tag{16}$$

Comparison with (14) gives the following relations between $(p; q)$ and the spherical and cylindrical coordinates with axis along \mathbf{a} :

$$p^2 - q^2 = r^2 - a^2; \quad pq = a \cos \theta = az \tag{17}$$

and

$$\begin{aligned} a^2 - z^2 &= a^2 (r^2 - z^2) = a^2 (a^2 + p^2 - q^2) - p^2 q^2 \\ &= (a^2 + p^2)(a^2 - q^2); \end{aligned} \tag{18}$$

It follows that the real and imaginary parts of \mathfrak{r} are bounded by r and a , respectively:

$$\begin{aligned} p^2 &\leq r^2; \quad \text{i.e., } |\operatorname{Re} \mathfrak{r}| \leq |\operatorname{Re} \mathfrak{r}| \\ q^2 &\leq a^2; \quad \text{i.e., } |\operatorname{Im} \mathfrak{r}| \leq |\operatorname{Im} \mathfrak{r}| \end{aligned} \tag{19}$$

with equalities attained only when \mathbf{r} is parallel or antiparallel to \mathbf{a} .

Since \mathbf{a} will be a fixed nonzero vector throughout, we will usually regard $\mathfrak{r}; p; q$ as functions of r only, suppressing the dependence on \mathbf{a} . Note that $\mathbb{R}^3 - C$ is multiply connected since a closed loop that threads C cannot be shrunk continuously to a point without intersecting C . In particular, if we continue \mathfrak{r} analytically around a simple closed loop, we obtain the value $-\mathfrak{r}$ instead of \mathfrak{r} upon returning to the starting point. Thus \mathfrak{r} is a double-valued

¹ In \mathbb{R}^n , C would be a sphere of codimension 2 orthogonal to \mathbf{a} .

function on \mathbb{R}^3 . To make it single-valued, we choose a branch cut that must be crossed to close the loop. Instead of returning to the starting point as r , the sign reversal now takes place upon crossing the cut. To give an extension of the positive distance, the branch must be chosen so that

$$a \neq 0 \implies r \neq +r; \tag{20}$$

and the simplest such choice is obtained by requiring

$$\text{Re } r = p \geq 0; \tag{21}$$

The resulting branch cut consists of the disk spanning the circle C ,

$$D = \{r \in \mathbb{R}^3 : p = 0, q = r - a; r - a = 0\}; \quad @D = C; \tag{22}$$

D will be called the standard branch cut and r the standard complex distance. General branch cuts, obtained by deforming D while leaving its boundary intact, will be considered in the next section.

If the observer is far from C , it follows from (14) and (20) that

$$r - a \approx p - r \text{ and } q \approx a \cos \theta; \tag{23}$$

Thus, $(p; q=a)$ are deformations of the spherical coordinates $(r; \cos \theta)$ near the source. From (17) and (18) it follows that level surfaces of p^2 (as a function of r , keeping $a \neq 0$ fixed) are spheroids S_p and those of q^2 are the orthogonal hyperboloids H_q , given by

$$S_p : \frac{r^2}{p^2 + a^2} + \frac{z^2}{p^2} = 1; \quad p \neq 0 \tag{24}$$

$$H_q : \frac{r^2}{q^2 - a^2} - \frac{z^2}{q^2} = 1; \quad 0 < q^2 < a^2; \tag{25}$$

All these quadrics are confocal with C as the common focal set. As $p \rightarrow 0$, S_p collapses to a double cover of the disk D . The variables $(p; q)$, together with the azimuthal angle about the a -axis, determine an oblate spheroidal coordinate system, as depicted in Figure 1.

We now define the extended propagator as

$$\tilde{G}(r; t) = \frac{\tilde{G}(r)}{r} = \frac{1}{2i\pi(\tilde{G}(r))}; \tag{26}$$

This is our basic wavelet,² from which the entire wavelet family is obtained by spacetime translations:

$$\tilde{G}_z(x) = \tilde{G}(x - z); \quad z = x^0 + iy = (x^0 + ia; t^0 + ib) \in \mathbb{T} \tag{27}$$

² In applications, it is better to use time derivatives of \tilde{G} , which have vanishing moments and better temporal decay and propagation properties [K 4].

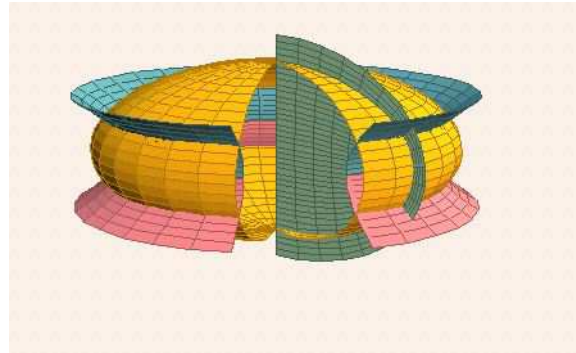


Fig. 1. The level surfaces of p, q and r form an oblate spheroidal coordinate system.

The family G_z may be called eigenwavelets of the wave equation in the sense that they are proper to that equation, though of course they are not eigenfunctions. In fact, $G_z(x)$ is seen [K 3] to be a pulsed beam originating from $r = r^0$ at $t = t^0$ and propagating along the direction of $a=b$, i.e., along a if y is in the future cone and along a if y is in the past cone. The pulse has a duration $|b|$ along the beam axis. By letting y approach the light cone ($a \rightarrow |b|$), the beam can be focused as tightly as desired around its axis, approximating a single ray along y . Equation (10) states that the extended causal solution $f(x \rightarrow iy)$ is a superposition of eigenwavelets, all with the same y . This gives a directional scale analysis of the original solution $f(x)$ which may be called its eigenwavelet transform.

The eigenwavelets have the spheroids S_p as wave fronts and propagate out along the orthogonal hyperboloids H_q with strength decaying monotonically away from the front beam axis. Hence they have no sidelobes, which makes them potentially useful for applications to communication, radar and related areas. These properties are illustrated in Figures 2 and 3.

We may visualize the effects of the extension $G(r; t) \rightarrow G(r; \tau)$ as follows. The extension $t \rightarrow \tau$ replaces the spherical impulse $(t - r)$ in (6) by a spherical pulse $\sim \delta(\tau - r)$ of duration $|b|$. The extension $r \rightarrow r$ then deforms this spherical pulse to a pulsed beam in the direction of $a=b$. By (23),

$$r = a + r \cos \theta; \tag{28}$$

hence the larger we choose a , the stronger the dependence of r on $\cos \theta$ in the far zone and the more focused the beam.

Let us emphasize that G depends on the complex spatial vector $r \in \mathbb{C}^3$ only through the complex distance r by writing

$$(r; \tau) = G(r; \tau) = \frac{1}{2i\pi(\tau - r)}; \tag{29}$$

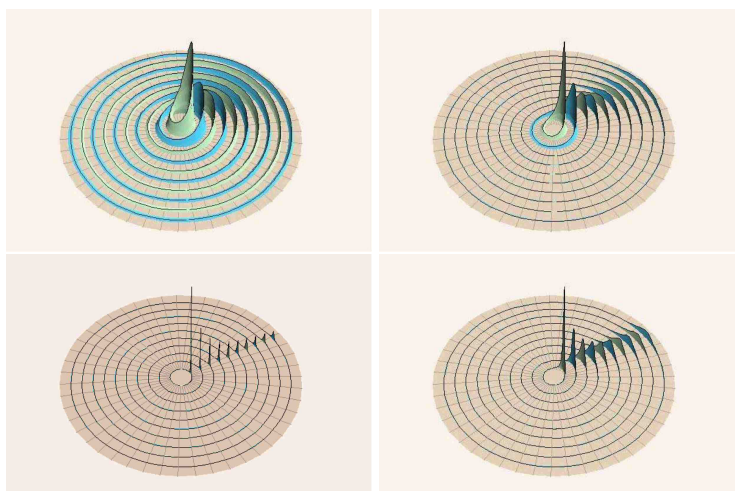


Fig. 2. Time-lapse plots of $\tilde{f}(x - iy)$ in the far zone, showing the evolution of a single pulse with propagation vector $y = (0; 0; a; b)$. Clockwise from upper left: $b/a = 1.5; 1.1; 1.01; 1.0001$. As $b/a \rightarrow 1$, y approaches the light cone and the pulsed beam becomes more and more focused around the ray y . We have taken the slice $x_2 = 0$, so that the disk D becomes the interval $[-a; a]$ on the x_1 -axis and the pulse propagates in the x_3 direction of the $x_1 - x_3$ plane.

Due to the factor r in the denominator, \tilde{f} is discontinuous across D and singular on C . D generalizes the point singularity of G at $r = 0$ and will be the spatial support of the source (9). To avoid further singularities, the factor

$$r = (t - p) - i(b - q)$$

must not vanish for any r . By (19),

$$b - q \neq 0 \text{ } \forall r, \quad a < |b| \tag{30}$$

so a necessary and sufficient condition for $(\tilde{f}; t)$ to be analytic whenever $r \notin D$ is that $(\tilde{f}; t) \in \mathcal{D}'$. Recalling that the tightness of the beam is controlled by the size of a , (30) means that the beam cannot become tighter than a single ray and, in fact, fails to be analytic along the ray in the limit $a = |b|$.

The volume element in \mathbb{R}^3 in oblate spheroidal coordinates is

$$dV = \frac{1}{a} (p^2 + q^2) dp dq d\phi = \frac{1}{a} \tilde{r}^2 dp dq d\phi; \tag{31}$$

hence \tilde{f} is locally integrable and square integrable. A differentiation gives

$$\Delta \tilde{f}(x - iy) - \tilde{f}(x - iy) = 0 \quad (x - iy \in \mathbb{R}^3; r \notin D); \tag{32}$$

Therefore $\tilde{f}(x - iy)$, with y a fixed timelike vector, is a distribution in $x = (r; t)$ with spatial support in D . (The temporal support is noncompact; in fact, $\tilde{f}(x - iy)$ decays as $1/r$ due to the Cauchy kernel.)

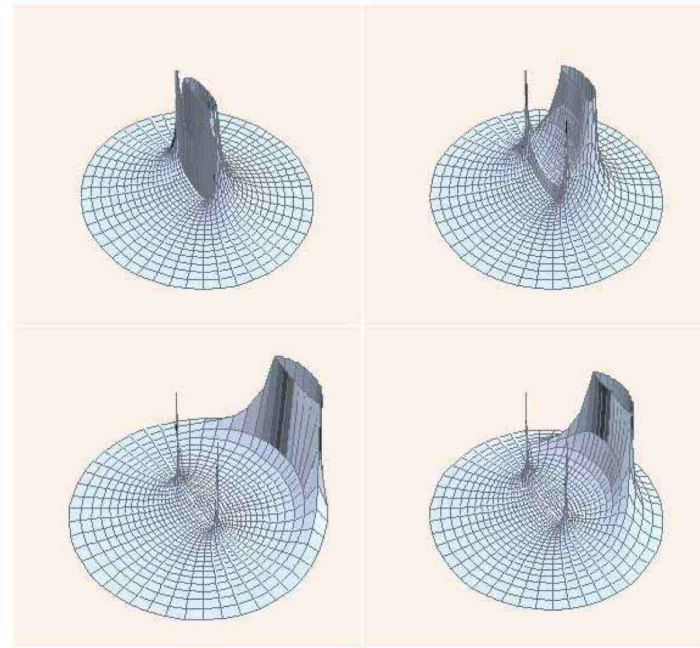


Fig. 3. Near-zone graphs of $f^2(x - iy)^2$ with $y = (0; 0; 1; 1; 0.1)$ immediately after launch, evolving in the x_1 - x_3 plane with $x_2 = 0$ as in Fig. 1. Clockwise from upper left: $t = 0.1; 1; 2; 3$. The ellipsoidal wave fronts and hyperbolic flow lines are visible. The top of the peak is cut off to show the behavior near the base. The two spikes represent the branch circle, whose slice with $x_2 = 0$ consists of the points $(\pm 1; 0; 0)$.

The source $\tilde{u}(x - iy)$ was computed explicitly in [K3] and turns out to be quite singular. It consists of a single layer and a double layer on D , both of which diverge on the boundary C where \tilde{u} is singular. We will compute regularized versions of \tilde{u} and \tilde{v} by using the freedom to deform the branch cut to eliminate the singularity on C .

3 Regularization by branch cut deformation

A general branch cut B is a membrane obtained by a continuous deformation of the disk D leaving its boundary intact,

$$\partial B = C: \tag{33}$$

B inherits an orientation from D , which in turn is oriented by a . Let V_B be the compact volume swept out in the deformation from D to B . Let us define the complex distance \mathfrak{r}_B with branch cut B in terms of $r = \mathfrak{r}_B$ by

$$\epsilon_B = \begin{cases} \epsilon & \text{if } r \notin V_B \\ \epsilon & \text{if } r \in V_B : \end{cases} \quad (34)$$

I claim that ϵ_B is continuous except for a sign reversal across B , generalizing the sign reversal of ϵ across D . This can be seen most simply if B does not intersect the interior of D , so that they have only the boundary in common. Then V_B is either all on the 'positive' or all on the 'negative' side of D . If V_B is 'positive,' then its boundary is

$$\partial V_B = B \cup D ; \quad (35)$$

meaning that the orientation (outward normal) of the boundary is positive on B and negative on D . Since ϵ changes sign upon crossing D 'upward' into V_B , (34) shows that ϵ_B is continuous across D . This proves that its only discontinuity is the sign reversal in crossing B , as claimed. Similarly, if V_B is 'negative,' then its boundary is

$$\partial V_B = D \cup B \quad (36)$$

and the above argument remains valid. To handle branch cuts that intersect the interior of D , we restate the 'negative' case (36) by declaring V_B negatively oriented, so that its boundary is oriented by the inward normal. Denoting the negatively oriented volume by \bar{V}_B , (36) can be restated as

$$\partial(\bar{V}_B) = B \cup D : \quad (37)$$

Hence the rule (35) applies to every branch cut B obtained by a continuous deformation of D , whether or not it intersects the interior of D , provided the orientation of the swept-out volume is taken into account. If B intersects the interior of D , then V_B has both positively and negatively oriented components. The definition §4) of the branch ϵ_B remains valid whether V_B (or any of its components) is positively or negatively oriented.

Of special interest will be the upper and lower spheroidal branch cuts

$$B = S \cup A \quad (38)$$

where S denote the upper and lower hemispheroids

$$S = \{r \in S : z > 0\}$$

and

$$A = \{r : r^2 = a^2, z^2 = a^2 - r^2\}$$

is the apron connecting them to C , which must be included so that $\partial B = C$ as required. The cut B^+ is depicted in Figure 4.

We can now construct a regularized version of the extended propagator by taking the average of the propagators with cuts B^+ and B^- . Denote the complex distances with cuts B by ϵ instead of ϵ_B , and let

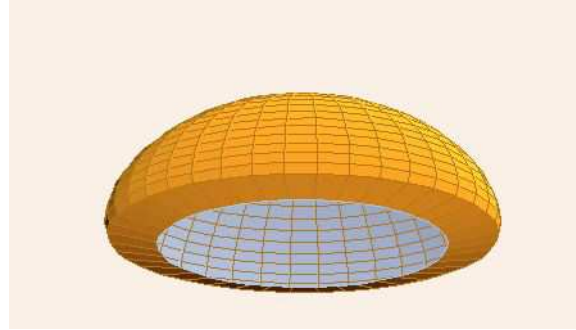


Fig. 4. The upper hemispherical branch cut B^+ with its apron.

$$A(x; t) = \frac{1}{2} (x; t) + (x; t) = G_A(x - iy): \quad (39)$$

Let V be the interiors of the upper and lower hemispheroids. By (34),

$$r \in V^+ \Rightarrow r_i = r; r = r \quad (40)$$

$$r \in V^- \Rightarrow r_i = r; r = r: \quad (41)$$

Hence, in both V we have

$$A(x; t) = \frac{1}{4 i r(t - r)} - \frac{1}{4 i r(t + r)} = \frac{1}{2 i(t^2 - r^2)}; \quad (42)$$

which is independent of the choice of branch. This shows that the discontinuities across the aprons cancel in the average A . Furthermore, by (30) we have

$$|j| > a \Rightarrow t^2 - r^2 = (t - r)(t + r) \notin 0;$$

showing that the singularities on C cancel as well. That is, A is analytic at all interior points of the spheroid S .

In the exterior of S we have $r = r$ and hence $A =$. Since D is contained in S and is analytic outside of D , we conclude that $A(x; t)$ fails to be analytic only when $r \in S$. Denoting the interior field by V_1 and the exterior field by V_2 , we have

$$\begin{aligned} V_1(x; t) &= \frac{1}{2} (x; t) + (x; t) \quad (43) \\ V_2(x; t) &= (x; t): \end{aligned}$$

Thus A is analytic except for a bounded jump discontinuity across S given by

$$J(x; t) = V_2(x; t) - V_1(x; t) = \frac{1}{2} (x; t) - (x; t) = G_J(x - iy): \quad (44)$$

It follows by the same argument as in (32) that the source distribution

$$4 \tilde{A}(x, iy) = x_A(x; t) \tag{45}$$

is supported spatially on S . Because \tilde{A} is obtained by twice differentiating a discontinuous function, it consists of a combination of single and double layers on S . But the jump discontinuity in A is bounded (unlike that in ψ , which diverges on C), and so are these layers; see [K 4].

The above arguments remain valid if instead of B we use any two branch cuts whose common interior V contains the branch circle C . In that case, the averaged propagator is analytic in T except for a finite discontinuity when r crosses the boundary ∂V , and its source distribution is supported spatially on ∂V . However, the above choice has the advantage that $\partial V = S$ are wave fronts, hence all parts of the surface radiate simultaneously and coherently.

4 Extended Huygens sources

Let H be the Heaviside step function. Since $0 < p < \infty$ in the interior of S and $p > \infty$ in the exterior, we have

$$A(x; t) = H(p - \infty) \psi_1(x; t) + H(p - \infty) \psi_2(x; t) \tag{46}$$

where the interior and exterior fields are given by (43). This can be used to compute the source distribution \tilde{A} defined in (45), and the result is sum of terms with factors $(p - \infty)$ and $\psi_0(p - \infty)$. The former are interpreted as single layers on S , and the latter as double layers.

An interesting practical question is whether the wavelets A , interpreted as acoustic pulsed beams, can be realized by manufacturing their sources. A similar question can be posed for their electromagnetic counterparts, which solve Maxwell's equations; see [K 4]. It is doubtful whether an acoustic source can be produced including double layers, and the problem becomes even more difficult in the electromagnetic case because the current density involves yet another derivative, hence a still higher layer [K 4a]. The multilayered structure is unavoidable as long as we insist on surface sources. We now propose a method for constructing solutions of the wave equation where the transition occurs in a shell instead of a surface. It will be simpler to present this method initially in a somewhat more general context.

Given a function $p(r; t)$ on R^{n+1} and two regular values $p_1 < p_2$ in its range, define two time-dependent surfaces and volumes in R^n by

$$S_1(t) = \text{fr} : p(r; t) = p_1; S_2(t) = \text{fr} : p(r; t) = p_2$$

$$V_1(t) = \text{fr} : p(r; t) < p_1; V_2(t) = \text{fr} : p(r; t) > p_2$$

Let $f_1; f_2$ be solutions of the wave equation in R^{n+1} with sources $g_1; g_2$:

$$f_k(r;t) = g_k; \quad k = 1, 2; \quad (47)$$

We want to construct an interpolated solution $f(r;t)$ such that

$$f(r;t) = f_k(r;t) \delta_{r^2} V_k(t) \quad (48)$$

and compute its source. This can be done by choosing functions $h_k(r;t)$ with

$$h_1(r;t) = \begin{cases} 1; & r^2 \in V_1(t) \\ 0; & r^2 \in V_2(t) \end{cases}; \quad h_2(r;t) = 1 - h_1(r;t) \quad (49)$$

and letting

$$f = h_1 f_1 + h_2 f_2 \quad h_k f_k \quad (50)$$

where the (Einstein) summation convention is used. The source of f is found to consist of two parts,

$$g = f = g_i + g_r; \quad (51)$$

where

$$g_i = h_k g_k \quad (52)$$

is an interpolated source and

$$g_r = 2h_k \dot{f}_k - 2r h_k - r_k f + (h_k) f_k \quad (\dot{f} - \partial f) \quad (53)$$

is a transitional source which, by (49), is supported on the transition shell

$$V_T(t) = \{r : p_1 \leq p(r;t) \leq p_2\} \quad (54)$$

and depends only on the jump field $f_j = f_2 - f_1$:

$$g_r = 2h_2 \dot{f}_j - 2r h_2 - r_j f + (h_2) f_j; \quad (55)$$

Now suppose that $V_1(t)$ and $V_T(t)$ are compact and we are given only one source g_2 , supported in $V_1(t)$. Letting f_2 be its causal field, our objective is to find an equivalent source g supported in $V_T(t)$ whose causal field f is identical with f_2 in $V_2(t)$. It suffices to choose any solution f_1 whose source g_1 is supported in $V_2(t)$, since the interpolated source (52) then vanishes and hence $g = g_r \cdot f_1$ is a sourceless internal field in $V_1(t)$, and the source g_r so constructed on $V_T(t)$ generalizes the idea of a Huygens source on a surface surrounding the support of g_2 . We may recover the latter by assuming that p is time-independent (hence so are S_k and V_k) and choosing $h_k(r)$ so that

$$\lim_{p_1 \rightarrow p_2} r h_2(r) = (p(r) - p_2) n(r)$$

where $n(r)$ is a field of orthogonal vectors on S_2 pointing into V_2 . The corresponding scheme in the electromagnetic case reduces to the usual boundary conditions on an interface between two media [K 4a].

Returning to $n = 3$ with $p = \text{Re } r$, let $f_k = r_k$ as in (43) and h_k be time-independent (e.g., functions of p only). A smoothed version of A (39) is

$$A^{\text{sm}} = h_1 r_1 + h_2 r_2: \quad (56)$$

Since r_k are sourceless in V_T , (51) gives the smoothed version of (45) as

$$4 \tilde{A}^{\text{sm}} = \nabla_x A^{\text{sm}} = 2r h_2 - r_J - (h_2)_J \quad (57)$$

where

$$r_J = \frac{1}{2} \frac{\partial}{\partial r} (r; t) \quad (r; t) = \frac{t}{2 i r (t^2 - r^2)}$$

is the jump field from V_1 to V_2 as in (44), but no longer restricted to a single spheroid S . If we now let $p_1 \neq p_2 = a$ and

$$h_1 = H(p); \quad h_2 = H(p);$$

then the transition becomes abrupt on S and A^{sm} becomes A (39). Since

$$\begin{aligned} r h_2 &= (p) r p \\ h_2 &= {}^0(p) \dot{r} p^2 + (p) p; \end{aligned}$$

equation (57) becomes

$$4 \tilde{A} = 2 (p) r p - \dot{r} (p) p_J - {}^0(p) \dot{r} p^2_J$$

displaying the aforementioned single and double layer structure on S . To get an explicit expression, use [K 4, Appendix]

$$\begin{aligned} r p &= \frac{pr + qa}{p^2 + q^2}; & p &= \frac{2p}{p^2 + q^2} \\ \dot{r} p^2 &= \frac{p^2 + a^2}{p^2 + q^2}; & r p - r q &= 0 \end{aligned}$$

and

$$r p - r_J = {}^0_J r p \quad r r = {}^0_J \dot{r} p^2$$

where 0_J is the complex derivative of $(r; t)$ with respect to r (keeping in mind that $(r; t)$ are analytic in r for $p > 0$),

$${}^0_J = \frac{\partial}{\partial r} r_J = \frac{t}{2 i r^2 (t^2 - r^2)^2}:$$

5 Conclusions

Although I have concentrated on the wave equation in four-dimensional Minkowski space $R^{3;1}$, similar considerations apply in $R^{n;1}$. In fact, the awkward extension of the propagator, using the Cauchy kernel in time but the complex distance in space, becomes much more natural when $G(r;t)$ is viewed as the retarded part of the analytic continuation of the fundamental solution $G_E(R)$ of Laplace's equation in Euclidean R^{n+1} [K0, K3], based on the complex distance

$$R = \sqrt{R^2 - t^2}; \quad R \in C^{n+1};$$

whose branch points form a sphere S^{n-1} in R^{n+1} of codimension 2 and radius $|Im R|$. The extended delta function $\tilde{G}_E(R)$,³ defined by applying the Laplacian in R to the extension $G_E(R)$, is supported on S^{n-1} for odd $n \geq 3$, but a branch cut, consisting of a 'membrane' bounded by S^{n-1} , is needed in all other cases.⁴ Given any test function f in R^{n+1} , the convolution

$$f(R) = \int_{R^{n+1}} \tilde{G}_E(R - R^0) f(R^0) dV(R^0) \quad (58)$$

defines an extension of f to C^{n+1} , non-holomorphic in general, whose restriction to the Minkowski subspace $R^{n;1}$, obtained by letting $R = (r;it)$, is a solution of the following initial-value problem for the wave equation:

$$(\partial_t^2 - \Delta_r) f(r;it) = 0 \quad (59)$$

$$f(r;0) = f(r;0) \quad (60)$$

$$(\partial_t - i\partial_b) f(r;b+it) \Big|_{b=t=0} = 0 \quad (61)$$

For odd $n \geq 3$, the proof of (59) is based on the fact that \tilde{G}_E is distributed uniformly on S^{n-1} and hence f is a spherical mean of f [J55]. This relates the support of \tilde{G}_E for odd $n \geq 3$ to Huygens principle. The other cases can be treated by applying a distributional version of Hadamard's method of descent.

Equation (61) states that $f(r;b+it)$ satisfies the Cauchy-Riemann equation in its last variable; but since this holds only at one point, it does not imply analyticity in b as it cannot since $f(r;b)$ need not have any analytic continuation in b . If one exists, it is indeed given by $f(r;b+it)$. This generalizes an old theorem by Paul Garabedian [G64, pp 191-202].

Acknowledgements

I thank Dr. Arje Nachman for his sustained support of my research, most recently through AFOSR Grant # FA 9550-04-1-0139.

³ The subscript distinguishes $\tilde{G}_E(R)$ from the Minkowskian $\tilde{G}(x)$ in (9).

⁴ This is because $G_E(R) = c_n R^{n-1}$ for $n \geq 2$ and $G_E = c_1 \log R$ for $n = 1$.

References

- BG 91. C A Berenstein and R Gay, *Complex Variables: An Introduction*. Springer-Verlag, New York, 1991
- BG 95. C A Berenstein and R Gay, *Complex Analysis and Special Topics in Harmonic Analysis*. Springer-Verlag, New York, 1995
- B 98. C A Berenstein, *Integral geometry, Radon transforms and complex analysis*, Springer-Verlag, *Lecture Notes in Math.* 1684, pp 1{33, 1998
- G 64. P R Garabedian, *Partial Differential Equations*. Chelsea, New York, 1964; AMS Chelsea, Providence, 1998
- J55. F John, *Plane Waves and Spherical Means*. Interscience, New York, 1955
- K 88. A Kaneko, *Introduction to Hyperfunctions*. Kluwer, 1988
- KS99. G Kato and D C Struppa, *Fundamentals of Algebraic Microlocal Analysis*. Marcel Dekker, 1999
- K 94. G Kaiser, *A Friendly Guide to Wavelets*. Birkhauser, Boston, 1994 (sixth printing, 1999)
- K 0. G Kaiser, *Complex-distance potential theory and hyperbolic equations*, in *Clord Analysis*, J Ryan and W Sprossig (editors) Birkhauser, Boston, 2000. <http://arxiv.org/abs/math-ph/9908031>
- K 3. G Kaiser, *Physical wavelets and their sources: Real physics in complex spacetime*. *Topical Review*, *Journal of Physics A: Mathematical and General* Vol. 36 No. 30 (2003) R29{R338.
- K 4. G Kaiser, *Making electromagnetic wavelets*. *J. Phys. A: Math. Gen.* 37:5929–5947, 2004. <http://arxiv.org/abs/math-ph/math-ph/0402006>
- K 4a. G Kaiser, *Making electromagnetic wavelets II: Spheroidal shell antennas*. *Preprint*, August 2004. <http://arxiv.org/abs/math-ph/0408055>